

Validation of Soft Classification Models using Partial Class Memberships: An Extended Concept of Sensitivity & Co. applied to the Grading of Astrocytoma Tissues

Claudia Beleites^{a,b,*}, Reiner Salzer^c, Valter Sergo^a

^aCenter of Excellence for Nanostructured Materials and Department of Engineering and Architecture, University of Trieste, Italy

^bDepartment of Spectroscopy and Imaging, Institute of Photonic Technology, Jena, Germany

^cDepartment of Chemistry and Food Chemistry, Dresden University of Technology, Dresden/Germany

Abstract

We use partial class memberships in soft classification to model uncertain labelling and mixtures of classes. Partial class memberships are not restricted to predictions, but may also occur in reference labels (ground truth, gold standard diagnosis) for training and validation data.

Classifier performance is usually expressed as fractions of the confusion matrix, such as sensitivity, specificity, negative and positive predictive values. We extend this concept to soft classification and discuss the bias and variance properties of the extended performance measures. Ambiguity in reference labels translates to differences between best-case, expected and worst-case performance. We show a second set of measures comparing expected and ideal performance which is closely related to regression performance, namely the root mean squared error RMSE and the mean absolute error MAE.

All calculations apply to classical crisp as well as to soft classification (partial class memberships as well as one-class classifiers). The proposed performance measures allow to test classifiers with actual borderline cases. In addition, hardening of e.g. posterior probabilities into class labels is not necessary, avoiding the corresponding information loss and increase in variance.

We implemented the proposed performance measures in R package “softclassval” which is available from CRAN and at <http://softclassval.r-forge.r-project.org>.

Our reasoning as well as the importance of partial memberships for chemometric classification is illustrated by a real-word application: astrocytoma brain tumor tissue grading (80 patients, 37 000 spectra) for finding surgical excision borders. As borderline cases are the actual target of the analytical technique, samples which are diagnosed to be borderline cases must be included in the validation.

Keywords: soft classification, partial class membership, classifier validation, borderline cases ambiguous reference, biomedical spectroscopy

Accepted Author Manuscript

NOTICE: this is the author’s version of a work that was accepted for publication in Chemometrics and Intelligent Laboratory Systems. Changes resulting from the publishing process, such as peer review, editing, corrections, structural formatting, and other quality control mechanisms may not be reflected in this document. Changes may have been made to this work since it was submitted for publication. A definitive version was subsequently published in Chemometrics and Intelligent Laboratory Systems, 122 (2013), 12 – 22, <http://dx.doi.org/10.1016/j.chemolab.2012.12.003>.

The manuscript is also available at <http://arxiv.org/abs/1301.0264>, including the supplementary figures and tables.

Notation

Throughout this paper, we use the following symbols:

Symbol	Meaning
n, n_g	number of samples and classes, respectively
$G \in \{1, \dots, n_g\}$	crisp class (label)
$g \in [0, 1]^{n_g}$	class membership (row) vector
$\mathbf{G}^{(n \times n_g)}$	matrix of class memberships
p, r instead of g	distinguish prediction and reference
$\mathbf{Z}^{(n_g \text{ ref.} \times n_g \text{ pred.)}$	confusion matrix for n samples
$Z(p, r)$	function to calculate elements of \mathbf{Z} for single samples
$\Delta^{(n_g \text{ ref.} \times n_g \text{ pred.)}$	residual confusion matrix
$\text{Sens}_G^{\text{operator}}$	sensitivity wrt. class G , calculated using <i>operator</i>
\wedge	conjunction (AND-operator)
\neg	negation (NOT-operator)

1. Introduction

Validation of chemometric models is a crucial step: it is not enough to train a good model, but its quality actually needs to be demonstrated with representative test samples. Thus, one firstly needs a plan for obtaining suitable test samples and decide whether e.g. cross validation is appropriate, or whether

*Corresponding author

Email addresses: Claudia.Beleites@ipht-jena.de
(Claudia Beleites), reiner.salzer@chemie.tu-dresden.de
(Reiner Salzer), sergo@units.it (Valter Sergo)

unknown future samples are needed. An excellent discussion of such considerations is given by Esbensen and Geladi [1]. Secondly, the performance on the basis of the results is described by suitable quantitative measures, such as the root mean squared error (RMSE) in calibration or sensitivity, specificity and the like for classifiers.

This paper focusses on the second aspect, although the motivation for this study did arise from the first requirement. In the following section, we introduce a tumor tissue grading application where representative test sets need to include ambiguous samples, *i. e.* samples that according to the reference labelling (ground truth, gold standard diagnosis) partially belong to more than one class. We then show how to extend well-known classifier performance measures to work with partial class memberships in the reference labels. We next apply these to our tumor classifier, and finally discuss some more properties of the extended performance measures when applied to test samples that are unambiguously assigned to their class by the reference labels.

1.1. Application: Grading of Astrocytoma Tissues

We illustrate the use of partial memberships with a biospectroscopic three class classification problem. A detailed description of the application, including experimental details and spectroscopic interpretation, has already been published [2]. Briefly, gliomas are the most common primary brain tumors. Among them, the astrocytomas are the largest subgroup. The world health organization (WHO) distinguishes four grades of astrocytomas according to their histology and clinical behavior [3–5]. Astrocytomas °II tend to further de-differentiate and gain in malignancy. Astrocytomas °III are malignant, and glioblastomas (°IV; GBM) are the most undifferentiated gliomas. Astrocytomas °III and GBM can originate from lower grade tumors, or appear *de novo* [3, 6]. Pilocytic astrocytoma (°I) are predominantly juvenile and clinically distinct tumors and are *not* considered here.

Glioma treatment includes surgical excision, if possible. The complete removal of the tumor is one of the most important factors for the prediction of the recurrence-free survival time of the patient [6, 7]. Böker [8] reports that complete removal under surgical microscope reduces the number of tumour cells by 90–95 %, still leaving about 10^{10} tumour cells in the patient’s brain. Tumor surgery outside the brain often applies ample safety margins around the tumor to ensure that all tumour cells are removed. This is not possible in brain surgery as the normal brain tissue *must* be preserved. An additional difficulty arises from the infiltrative growth of the gliomas: the tumor border is hardly visible. Within 2 cm distance from the solid tumour, still about 10 % of the cells are tumour cells and even more than 4 cm outside the solid tumor glioma cells are found [8]. Thus, although complete removal of the tumor is desired, the surgeon often decides to remove only the malignant part of the tumor. Stereo-navigation based on pre-operative imaging such as magnetic resonance tomography (MRT) is used routinely to delineate the excision border, but the precision is limited by the brain shift during surgery. This constitutes the need for addi-

tional tools that help surgeons in finding the proper excision border *in-situ* and *in-vivo*.

The WHO grading scheme lists (morphological) properties of tissues. Conceptually, it is a traditional classification system in the sense that a set of classes is defined, and each sample belongs to exactly one of the classes. The tumor-biological reality, however, is not as distinct as the WHO grading scheme and changes at the molecular level do not necessarily occur at the same time as the changes in the morphology diagnosed during histological grading of the tumors [9, 10]. Neuropathologists frequently spot areas where cells are actually in the process of de-differentiation, *i. e.* in the transition from one class to the next. This leads to ambiguity in the description of those areas.

Another type of ambiguous diagnosis states that a tissue consists of a mixture of cells of different grades, *e. g.* tumor cells infiltrating normal tissue. This ambiguity can occur if the measurements spatially do not resolve cells. Diagnosis at single cell level, however, is not practical for intra-surgical guidance. The working precision of the surgeons (up to ca. 1 mm) requires corresponding spatial resolution of the diagnostic tool: too high spatial resolution not only means longer measurement times and/or undersampling but also confronts the surgeon with too detailed information in a time-critical situation.

Both types of ambiguity occur in our example application, grading of brain tumor tissue for *intra-surgical* decision. Note however, that grading of the actually measured tissue is different and easier than grading of the patient’s tumor. A detailed discussion of the differences between these two distinct grading tasks has been given in [2].

1.2. Crisp and Soft Classification

Crisp classification requires each sample to belong to exactly one of the n_g pre-defined classes. This restriction can be relaxed in two independent ways.

Multiple membership: A sample may belong to *more than* one class (or no class at all).

Partial membership: A sample may belong *partially* to any given class.

Multiple membership is often associated with one-class classifiers. One-class classifiers model each class independently of the other classes [11–13]. While this is not the case in our application (the tissue classes are mutually exclusive) the reasoning presented here works for one-class classifiers as well. We refer to the boundary condition of crisp classifiers that each sample must belong to exactly one class as “closed world”. “Open world” intermediate results can be transformed in closed world results by “winner takes all” or soft max (for partial memberships) rules.

The second concept is in analogy to the transition from hard (crisp) cluster analysis to fuzzy cluster analysis: the degree of belonging to a class is represented by a continuous membership value. In the remote sensing community, the term *soft classification* has already been established for such partial class memberships [14–18], so we adapt this terminology. Also, *fuzzy* usually refers to ambiguity as opposed to uncertainty, but the partial memberships can denote both. Partial class memberships

can be treated as intermediate results which are then “hardened” into crisp class memberships.

In chemometric *modelling*, the term “soft” is often used in different ways. Hard vs. soft modelling can refer to the amount of prior knowledge that is reflected in the model equations. While hard models fit equations that are derived from strong assumptions or first principles (*e.g.* order of reaction for kinetic studies), soft models make less assumptions and model empiric approximations (*e.g.* fitting some sigmoid) [19, 20]. The “soft” in Soft Independent Modelling of Class Analogies (SIMCA) comes from this distinction. SIMCA is an established and widespread one-class classification model, see *e.g.* [12, 21, 22] that has also been used in the context of vibrational spectroscopic diagnosis or distinction of biological tissues [23, 24] and cells [25]. Varmuza and Filzmoser [21], however, seem to use the term “soft” synonymous for one-class classifiers and Brereton [11] defines “soft” as allowing overlap in the (feature) space assigned to each class. “Soft” takes yet another meaning for soft margins of support vector machines (SVM) where soft margins allow samples in between the margins of the SVM in feature space, even though they are labelled as belonging to exactly one class [26].

In contrast to these soft aspects of chemometric models, we use the term *soft* in this paper with respect to class labels, and contrast it to *crisp*. The performance measures we discuss in the present paper therefore work regardless of these various soft aspects of classification models: validation usually treats the classifier as a black box that calculates class membership from the spectrum (feature vector) of a test sample. Our performance measures can be calculated just the same way whether the classifier uses hard or soft modelling, models classes independently or in distinction of the other classes, or whether it is a SVM with or without soft margin.

While partial memberships are widely used in cluster analysis (fuzzy c-means clustering is well established for the analysis of spectra of biological tissues [27–30]), this is not the case for chemometric classification. Classification addresses qualitative questions. But qualitative analysis is usually carried out by chemometric quantification (regression) which is then evaluated with respect to a threshold or limit. Calibration models adequately cover chemical composition, but are not appropriate for many bio-spectroscopic classification problems.

We employ (row) vectors $g \in \{0, 1\}^{n_g}$ with the elements corresponding to the sample’s class $g_G = 1$ and all other elements 0 to express the crisp class membership of a sample, which can be combined into a membership matrix with each row corresponding to one sample. We will use the term “crisp” label or sample also for samples that *happen* to have all class memberships either 0 or 1, and “soft” for samples where at least one membership value is not exactly 0 or 1. Thus, there may be (and often are) crisp samples also in a soft data set. The boundary condition for closed-world classifiers is $\sum_{j=1}^{n_g} g_j = 1$. Partial memberships allow the elements of g to take any value between 0 and 1: $g \in [0, 1]^{n_g}$.

Partial memberships can arise from two different concepts:

probability or uncertainty: This is common for predictions

like posterior probabilities, but may also be the case for reference labels.

mixtures of the underlying classes as in homogeneous mixtures or heterogeneous mixtures where the heterogeneity is not resolved by the measurement. In chemistry, this is closely related to the concept of concentration and thus to calibration. Non-chemical fields frequently use fuzzy set theory.

In practice both aspects can arise for one and the same problem. In biomedical applications, uncertain references arise *e.g.* from the pathologist expressing uncertainty: “there may be tumor cells between these normal cells”, or from disagreement among a panel of pathologists. In our experiments, the transfer of the histological diagnosis onto the measurement of a parallel section is an additional source of uncertainty. Our samples also contain two different types of mixtures: firstly, a tissue may consist of cells of different cell types, while the individual cells are not resolved by the measurement’s spatial resolution. The second type of mixture are currently de-differentiating tissues, *e.g.* cells undergoing the transition from °II to °III, which are therefore between the ordered classes.

Partial class memberships in classification may be used and discussed at three levels:

Soft predictions are widely used: posterior probabilities of linear or quadratic discriminant analysis (LDA and QDA) or logistic regression (LR); the voting proportion of k nearest neighbors (kNN), random forests, etc. Soft predictions are frequently considered an intermediate result and are then hardened by thresholds.

Soft training samples can be used by methods like LR, artificial neural networks or partial least squares discriminant analysis, PLS-DA), but up to now this is rarely done.

Soft test samples, *i.e.* samples with ambiguous or uncertain reference (ground truth, gold standard diagnosis) are the topic of this paper.

For classifier training, traditionally either crisp reference labels are enforced and/or borderline cases¹ are excluded. This raises several issues that are avoided by allowing soft labels. Hardening of a continuous variable implies a loss of information. Dichotomization of a logistically distributed random variable deletes at least 25 % of the information [31]. In biomedical spectroscopy, crisp reference labels are often enforced by requesting the pathologist to assign the sample to exactly one of the classes, even if the pathologist describes the sample as currently undergoing de-differentiation or consisting of mixed cell populations. In practice, the pathologist refuses to diagnose certain samples unambiguously (leading to exclusion of

¹Here, we use the terms borderline case and ambiguous sample synonymously and exclusively with respect to the true class membership. Spectra that are spectroscopically in between the typical spectra of classes will be referred to as “close to the class boundary”.

the sample). For other samples the written-out diagnosis contains information about the ambiguity that is not reflected by the assigned crisp class. The same applies to diagnoses given by a panel of pathologists. Again, either the majority class is used (removing the information contained in the disagreement) or the case is excluded. For the brain tumour patients, crisp diagnoses given by the local neuropathologist and neuropathologists from the tumour reference center often differ more than the written-out diagnoses. This is in accordance with hardening as possible cause of further variance. Likewise, the results of the panel diagnosis published by Kendall *et al.* [32] have higher discrepancy for intermediate classes [2].

In any case, one either uses possibly inappropriate descriptions as reference or gold standard diagnosis, or reduces the available number of samples. In bio-spectroscopy, where frequently hundreds or thousands of variates are measured for tens of patients only, this is a critical issue. In our application, $\frac{1}{3}$ of the patients and almost half of the spectra would have to be excluded. Moreover, excluding borderline samples comes at the risk of overestimating class separation: throwing away all difficult cases creates an easy problem. While such filtering and the corresponding output of “no certain prediction possible” are appropriate for certain analytical tasks, this is not the case in our application. Borderline samples are actual examples of the class boundaries. Excluding them from classifier training means excluding most valuable samples. The more so in our application, as these are also examples of the actual target samples of the glioma grading technique.

While one may also arrive at a good classifier with completely unambiguous training data, the validation must use carefully collected test samples: samples representative for the field of use. For our astrocytoma application these, again, are the borderline cases. Validation methods for soft labeled samples are thus even more crucial than the respective training strategies.

The remote sensing community has been using soft classification for a long time to describe the mixtures due to low spatial resolution. Proposals for validation of soft classifiers are reported in the literature [14–16]—yet, it is still considered an unsolved problem [17, 18]. We critically discuss these proposals below.

2. Classifier Performance: the Confusion Matrix and fractions thereof

For convenience, we abbreviate sums of particular parts of the confusion matrix \mathbf{Z} as follows: summation includes all possible indices according to the conditions written in the indices. *E. g.* $\sum \mathbf{Z}_{i,P}$ stands for $\sum_{i=1}^{n_g} \mathbf{Z}_{i,P}$ (sum all elements of column P), $\sum \mathbf{Z}_{i \neq G,P}$ means $\sum_{i \in \{1, \dots, n_g, i \neq G\}} \mathbf{Z}_{i,P}$ (sum all elements except that in row G of column P). \sum_n is the sum over all samples.

2.1. Hard Classification

The validation results of a crisp classifier are usually tabulated in the confusion matrix \mathbf{Z} . This matrix (fig. 1a) counts how many samples that truly belong to each class (rows) were

predicted to belong to that class (columns). In other words, a sample belonging to class R and predicted to belong to class P is counted in $\mathbf{Z}_{R,P}$. Sometimes, a notation as function of prediction and reference is more convenient:

$$\mathbf{Z}_{i,j} = \sum_n \mathbf{Z}(r_i, p_j) = \sum_n r_i \wedge p_j. \quad (1)$$

where \wedge stands for the AND operator which returns 1 if and only if both reference class membership r_i and prediction class membership p_j are 1, otherwise the return value is 0. In order not to clutter the notation, we indicate the sum over all samples by \sum_n without introducing an index for the sample. The symbol \mathbf{Z} for the confusion matrix will imply that this sum is already taken, whereas $\mathbf{Z}(r_i, p_j)$ is evaluated for each sample. The results are then summed up to give $\mathbf{Z}_{i,j}$.

Confusion matrices are frequently pooled (*e. g.* k confusion matrices obtained during one iteration of k -fold cross validation are fused into one by matrix addition). Confusion matrices yield a very detailed overview of a classifier’s performance. Frequently, the confusion matrix is further summarized by proportions calculated thereof. These proportions (fig. 1b – 1e) answer questions with regard to the predictive abilities of a classifier. Different disciplines refer to these fractions differently. We use the medical terminology [33, 34]:

Sensitivity Sens_G : How well does the classifier recognize samples of class G ?

Specificity Spec_G : How well does the classifier recognize that a sample does *not* belong to class G ?

Positive Predictive Value PPV_G : Given the prediction is class G , what is the probability that the sample truly belongs to G ?

Negative Predictive Value NPV_G : Given a prediction “does not belong to class G ”, what is the probability that the sample truly does not belong to G ?

Note that the predictive values are the “inverse” (as in inverse calibration) of sensitivity and specificity: sensitivity and specificity report the distribution of test outcomes as function of the true disease status. In contrast, the predictive values give the distribution of true disease status as function of the observed test outcome.

For users of the classifier, the predictive values are usually of more interest than sensitivity and specificity: patients and doctors want to know whether *this particular* patient is ill rather than whether the test can recognize ill people; manufacturers want to know whether a product can be sold rather than whether bad batches can be found. Answering these questions needs to take into account the prior probabilities of the classes (in medical diagnosis: prevalence). The relative frequencies of the classes in the test set (row sums of the confusion matrix \mathbf{Z}) do *not* necessarily reflect the prior probabilities. Moreover, the prior probabilities can vary greatly among different populations (consider *e. g.* HIV tests for blood donors and drug addicts, respectively). The reported predictive values should therefore

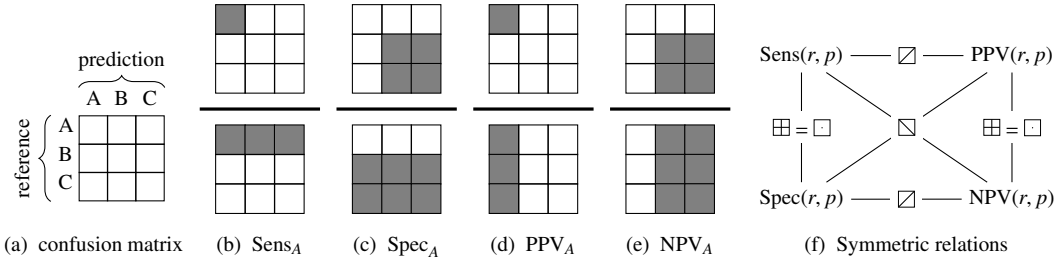


Figure 1: Confusion matrix (a) and characteristic fractions for sum constrained multi class classifiers (b) – (e). The parts of the confusion matrix summed as numerator and denominator for the respective fraction with respect to class A are shaded. (f) Symmetry between the measures. $\boxplus = \boxminus$: mirror horizontally and vertically or at point $(r; p) \mapsto (1 - r; 1 - p)$, \boxtimes : mirror at major diagonal $(r; p) \mapsto (p; r)$, and \boxminus : mirror at minor diagonal $(r; p) \mapsto (1 - p; 1 - r)$. All symmetry elements with respect to the center of the value space at $(0.5; 0.5)$. The icons use Cartesian coordinates. (a) – (e) are reprinted from [?], with permission from Elsevier.

be corrected for the different composition of test set and target population and also specify the (assumed) composition of the target population. The same caution applies for all measures that combine different reference classes, such as overall accuracy, the chance agreement needed to calculate corrected performance values like the κ statistic, etc.

Usually, these performance measures relate to medical decisions whether a certain disease is present or absent. This corresponds to one-class classifiers. The questions translate to the following expressions:

$$\text{Sens}_G = \frac{\mathbf{Z}_{G,G}}{\sum_n r_G} \quad (2)$$

$$\text{PPV}_G = \frac{\mathbf{Z}_{G,G}}{\sum_n p_G} \quad (3)$$

$$\text{Spec}_G = \frac{\mathbf{Z}_{-G,-G}}{\sum_n r_{-G}} \quad (4)$$

$$\text{NPV}_G = \frac{\mathbf{Z}_{-G,-G}}{\sum_n p_{-G}} \quad (5)$$

The membership g_{-G} of the dummy class “-G” (“not class G”) is obtained as $g_{-G} = 1 - g_G$. The same expressions can be used for closed-world classifiers, where the constraint in addition allows the alternative calculation as the sum of memberships to the other classes $g_{-G} = 1 - g_G = \sum_{g \neq G} g_g$, see fig. 1b – 1e.

In analogy to the addition of confusion matrices, the overall (multi-sample) performance is the average of the single sample performances weighted by the denominator variable.

Like the confusion matrix, also the performance measures can be written as function, and due to the symmetry between the performance measures (compare fig. 1f), all operators can be expressed using one basic underlying function. Performance measures as well as the class memberships refer to each class independently of the other classes for both one-class and closed-world classifiers. We drop the class index for convenience:

nience:

$$\text{Sens}(r, p) = \frac{\sum_n \mathbf{Z}(r, p)}{\sum_n r} \quad (6)$$

$$\text{Spec}(r, p) = \text{Sens}(1 - r, 1 - p) \quad (7)$$

$$\text{PPV}(r, p) = \text{Sens}(p, r) \quad (8)$$

$$\text{NPV}(r, p) = \text{Sens}(1 - p, 1 - r) \quad (9)$$

2.2. Soft Confusion Matrices

To generalize the confusion matrix and performance measures for soft reference and prediction, the Boolean AND-operator \wedge (conjunction) in the definition of the crisp confusion matrix (eq. 1) is replaced by a suitable operator for continuous-valued input in the range $[0, 1]$. The three main candidates are the minimum (weak conjunction), as proposed e. g. by Łukasiewicz and Gödel, the strong conjunction $\max(x + y - 1, 0)$ (Łukasiewicz), and the product [35–37]. These operators reflect the ambiguity in the performance estimate due to the ambiguity expressed by the soft memberships.

The rationale behind these operators can be illustrated by a situation where low (e. g. spatial) resolution causes the ambiguity (fig 2). Say, a number of cells are in the measurement volume of a spectrum, and half of them are cancer cells and the other half are normal. The classifier yields a fraction of 0.8 for cancerous. In the best case, the classifier recognized the cancerous half correctly, so the conjunction (overlap) for the “cancer” class is 0.5. In the worst case, the classifier assigns “cancer” to normal cells. However, since at least 0.3 must still be assigned to the correct “cancer” class, the overlap is 0.3. The true overlap can be anywhere between these bounds, depending on the true distribution of cancer cells and the distribution of cancer cells predicted by a high-resolution classifier. E. g. if they are uniformly randomly distributed, for each cell the chance that it is both cancerous and predicted to be cancerous is $0.5 \cdot 0.8 = 40\%$, and the expected overlap is 0.4 (middle column of fig 2). The top row of the supplementary figure S.1 illustrates the three operators as function of reference and predicted memberships, fig. 3 compares them for given reference memberships.

The *weak conjunction* is the standard AND-operator in fuzzy logic, and has been used to compute soft confusion matrices

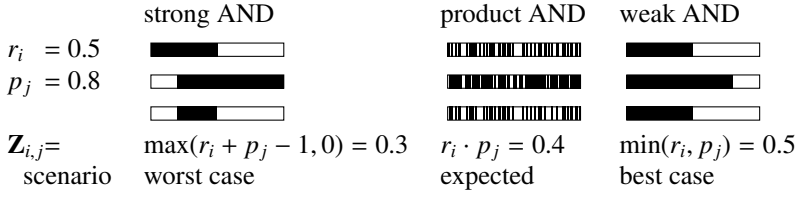


Figure 2: The soft AND-operators: hypothetical high-resolution scenarios corresponding to a low resolution situation with reference = 0.5 (top row) and prediction = 0.8 (middle row) membership to the black class. In each column, the overlap (bottom row) is obtained by the classical Boolean AND: for each position, $Z_{i,j, pos} = r_{i, pos} \wedge p_{j, pos}$, the soft conjunction is the fraction where both r_i AND p_j belong to the black class.

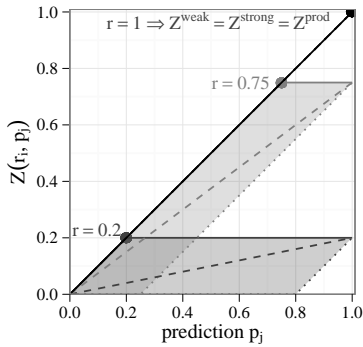


Figure 3: Behavior of the confusion matrix function $Z(r_i, p_j)$ for the three operators for reference memberships (points) $r_i = 1$ (black), 0.75 (light gray), and 0.2 (dark gray): Z^{weak} (upper bound of the parallelograms, continuous line), Z^{strong} (lower bound of the parallelograms, dotted line), and Z^{prod} (dashed line). For reference class membership $r_i = 1$ all three Z equal the predicted membership p_j .

[15].

$$Z^{\text{weak}}(r_i, p_j) = \min(r_i, p_j) \quad (10)$$

The minimum is the *highest* possible overlap between prediction and reference (best case scenario in fig. 2 and upper bound in fig. 3).

The *strong conjunction* has been introduced for soft classifier performance by Pontius *et al.* [38]. It reports the *lowest* possible overlap between reference and prediction (worst case scenario in fig. 2 and lower bound in fig. 3).

$$Z^{\text{strong}}(r_i, p_j) = \max(r_i + p_j - 1, 0) \quad (11)$$

As $\max(r_i + p_j - 1, 0) = r_j - \min(r_i, 1 - p_j)$, Z^{weak} and Z^{strong} are point symmetric about $(p = \frac{1}{2}; Z = \frac{1}{2}r)$ to each other (fig. 3).

The matrix diagonal of Z^{weak} reports the best possible performance that is in accordance with the given reference and prediction. Likewise, the off-diagonal elements are the worst possible performance for the respective type of misclassification $R \mapsto P$. Z^{strong} behaves antithetically.

Both Z^{weak} and Z^{strong} lack two properties of crisp confusion matrices that have been identified as desirable for soft confusion matrices [16, 17]: firstly, their marginal sums do not equal the reference and prediction class membership vectors. Sec-

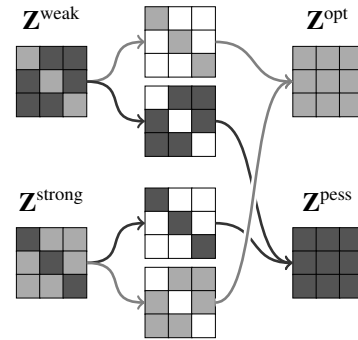


Figure 4: Recombination of Z^{weak} and Z^{strong} into Z^{opt} and Z^{pess} . The diagonal of Z^{weak} and the off-diagonal elements of Z^{strong} measure the best possible performance (light gray), while Z^{strong} 's diagonal and Z^{weak} 's off-diagonal elements report the worst case performance (dark gray). The resulting confusion matrices give the most optimistic and most pessimistic view on the classifier's performance in accordance with the given reference memberships and the observed predictions.

ondly, perfect reproduction does not produce a diagonal confusion matrix and is thus more difficult to recognize than in crisp classification problems.

Several proposals on how to “repair” both marginal sums and diagonal structure of Z^{weak} for perfect reproduction of the reference exist [16, 17, 38]. They all distribute the remainder of the prediction after the agreement (diagonal) has been subtracted. Again, diagonal and off-diagonal elements of these composite confusion matrices do not share the same interpretation. Silván-Cardenás and Wang [17] report that the use of soft confusion matrices in practice appears to be restricted to the diagonal of Z^{weak} , $Z^{\text{weak}}(r_G, p_G)$.

Interestingly, the properties of Z^{weak} and Z^{strong} have not yet been interpreted with respect to resulting bias of the performance measure. Using exclusively the diagonal of Z^{weak} results in a strong optimistic bias: only the “optimistic” part of Z^{weak} is used. We are not aware of any application where the corresponding pessimistic performance measures are reported, although Z^{strong} as a measure of the least possible overlap is mentioned (but not used) by Pontius *et al.* [38].

Using a performance measure that has by construction a strong optimistic bias, *i. e.* overestimates the classifier's per-

formance, is clearly not appropriate for an application where the classifier should ultimately indicate whether brain tissue is cut out or not. Similar caution is necessary in most biomedical and many chemometric applications.

We therefore propose to recombine \mathbf{Z}^{weak} and $\mathbf{Z}^{\text{strong}}$ into “optimistic” and “pessimistic” confusion matrices \mathbf{Z}^{opt} and \mathbf{Z}^{pess} as illustrated in fig. 4. These two matrices hold the best and worst possible performance for the observed test results, and can therefore be interpreted consistently without the need to distinguish diagonal and off-diagonal elements. Together, the two confusion matrices span the range of possible performances that is in accordance with the available reference (gold standard diagnosis) and the observed predictions. The ambiguity in the reference labels causes this uncertainty about the true performance: any performance in this range may be the true performance of the classifier. Due to the ambiguity or uncertainty in the reference labels, the true performance cannot be further narrowed down.

We define the performance measures (eqs. 6–9) so that only single elements from the diagonal of the confusion matrix \mathbf{Z} are needed to obtain these optimistic and pessimistic bounds.

The interpretation as best and worst possible performance does not take into account that the validation results are actually performance *estimates*. “Best” and “worst” here refer to the uncertainty due to the ambiguity represented by soft class memberships. The performance estimates are subject to additional uncertainty due to the sampling of the actual test set and possible instability of the “surrogate” models computed during cross validation etc. However, this is outside the scope of this paper.

The *product* has been used as AND-operator for continuous-valued logic as well, *e. g.* in Reichenbach’s probability logic [39], and has also been discussed for soft confusion matrices [16, 17, 38, 40]:

$$\mathbf{Z}^{\text{prod}}(r_i, p_j) = r_i \cdot p_j \quad (12)$$

Interpreting the class memberships as probabilities, \mathbf{Z}^{prod} gives the expected amount of coincidence for independent processes determining the class memberships. In the mixture interpretation, \mathbf{Z}^{prod} follows from the information loss due to low (spatial) resolution: assume crisp reference and prediction are available at high resolution, but the location information is lost (the high resolution data is mixed randomly). The expected confusion matrix (normalized by the respective number of samples) in this situation is just the product-based confusion matrix \mathbf{Z}^{prod} . From a Bayesian point of view, a uniform prior is used in both interpretations.

The marginal sums of the product-based confusion matrix \mathbf{Z}^{prod} behave like the marginal sums of the crisp confusion matrix, for closed world as well as for one-class classifiers: the row sums are $\sum_n(r \cdot \sum p)$ and the column sums are $\sum_n(p \cdot \sum r)$. The sum over all elements is $\sum_n \sum p \cdot \sum r$. Specifically, both marginal sums and the total element sum of \mathbf{Z}^{prod} equal the number of samples for closed world classifiers. However, like the other soft confusion matrices (except \mathbf{Z}^{opt}), \mathbf{Z}^{prod} is not diagonal if the prediction equals the soft reference. This may

be seen as expression of the remaining uncertainty or ambiguity arising either from the lack of further information about the (unresolved) distribution of the classes, or from the uncertainty encoded in both reference and prediction.

2.3. Calculating the Performance Measures for Soft Reference and Prediction.

Eqs. (6) to (8) can directly be used with the soft confusion matrices. Note that the performance measures refer only to diagonal elements of the confusion matrix \mathbf{Z} . Thus, all problems due to the marginal sums not equaling prediction and reference membership vectors are avoided, including possible specificities or negative predictive values >100% for \mathbf{Z}^{weak} . \mathbf{Z}^{weak} and $\mathbf{Z}^{\text{strong}}$ directly yield the most optimistic and most pessimistic case. Fig. S.1 illustrates the performance measures for the three different operators. Note that each pair of \mathbf{Z}^{weak} (optimistic) and $\mathbf{Z}^{\text{strong}}$ (pessimistic) leaves a quarter of the input space completely without information: if reference and prediction are too ambiguous, they are in accordance with any possible value of the performance measure (interval width in fig. S.1).

For the product operator, the four characteristic measures simplify to prediction, 1 - prediction, reference and 1 - reference for each sample and weighted averages thereof for the multi-sample performance.

The Difference between Prediction and Reference. The mixture interpretation of soft memberships suggests a treatment of soft classification analogous to regression.

Regression residuals measure the deviation of the prediction from the reference. A short inspection of the soft confusion matrices reveals that \mathbf{Z}^{weak} yields performance 1 if the prediction p equals (or exceeds) the reference r . This means that it inherently reports deviations from the ground truth or gold standard diagnosis (though only for too low estimates, too high estimates are not penalized). $\mathbf{Z}^{\text{strong}}$ produces a more complicated behavior (bottom row of fig. S.1).

In contrast, the resulting performance measures for the product operator simplify to the regression errors distributed according to the reference memberships: analogous to the calculation of regression residuals $\varepsilon = \hat{y} - y$, we compare the observed confusion matrix $\mathbf{Z}^{\text{prod}}(r, p)$ with the “ideal” confusion matrix for the actual reference $\mathbf{Z}^{\text{prod}}(r, p = r)$ [40]:

$$\Delta^{\text{prod}} = \mathbf{Z}^{\text{prod}}(r, p) - \mathbf{Z}^{\text{prod}}(r, r) \quad (13)$$

Just as for regression, the sign of the residuals distinguishes over- or underestimation. Thus we sum the absolute deviations rather than their signed values (squared deviations are discussed below). In closed world systems, every underestimation implies the same amount of overestimation in other classes: the row sums of Δ^{prod} are 0.

Also, Δ measures an error, so we compute the complementary $1 - |\Delta|$ as our performance measures refer to the correct

part of the prediction:

$$\text{Sens}^{\text{MAE}}(r, p) = 1 - \frac{\sum_n |\Delta^{\text{prod}}(r, p)|}{\sum_n r} \quad (14)$$

$$= 1 - \frac{\sum_n |Z^{\text{prod}}(r, p) - Z^{\text{prod}}(r, r)|}{\sum_n r} \quad (15)$$

$$= 1 - \sum_n \frac{r}{\sum_n r} |p - r| \quad (16)$$

Sens^{MAE} uses the mean absolute error weighted by the reference memberships (compare eq. 6). The specificity reports the remainder of the residuals, which is attributed to samples not belonging to the class:

$$\text{Spec}^{\text{MAE}}(r, p) = 1 - \sum_n \frac{1-r}{\sum_n 1-r} |p - r| \quad (17)$$

The predictive values characterize the inverse thought, consequently deviations are distributed according to the *predicted* memberships:

$$\text{PPV}^{\text{MAE}}(r, p) = 1 - \sum_n \frac{p}{\sum_n p} |p - r| \quad (18)$$

$$\text{NPV}^{\text{MAE}}(r, p) = 1 - \sum_n \frac{1-p}{\sum_n 1-p} |p - r| \quad (19)$$

Mean Absolute Error MAE and Root Mean Squared Error RMSE. Instead of the weighted MAEs, the respective RMSEs can be used, *e. g.*:

$$\text{Sens}^{\text{RMSE}}(r, p) = 1 - \sqrt{\sum_n \frac{r}{\sum_n r} (p - r)^2} \quad (20)$$

The MAE is more closely related to the usual error counting for crisp classifiers, while the RMSE is more common for regression models. For calculating the performance of soft prediction and crisp reference, the mean squared error MSE is also known as Brier score [41].

MAE and RMSE are related: In general, $\text{MAE} \leq \text{RMSE} \leq \sqrt{n} \text{MAE}$ with the respective number of samples n . For classification, however, no single prediction can deviate by more than 1 from the reference (and this only for crisp reference memberships): $0 \leq \text{MAE} \leq 1$. Thus, $\text{MAE} \leq \text{RMSE} \leq \sqrt{\text{MAE}}$. For soft reference, the upper bounds of both MAE and RMSE are lower, as the maximal deviation is the greater of r and $1 - r$, respectively, for each sample. Fig. 5 illustrates the bounds for crisp reference data as well as for our application.

Inter-class performance. Δ^{prod} and the derived performance measures count both under- and overestimations. This yields the expected behavior for class-wise performance measures. Performance measures that summarize more than one class (*e. g.* overall accuracy) should either take care of the consequences beforehand, or they may be normalized according to the maximal possible error. Closed world classifiers have one under- and one overestimation for each misclassification, thus $\text{MAE} \leq 2$ and $\text{RMSE} \leq \sqrt{2}$. For one-class classification the bounds are $\text{MAE} \leq n_g$ and $\text{RMSE} \leq \sqrt{n_g}$.

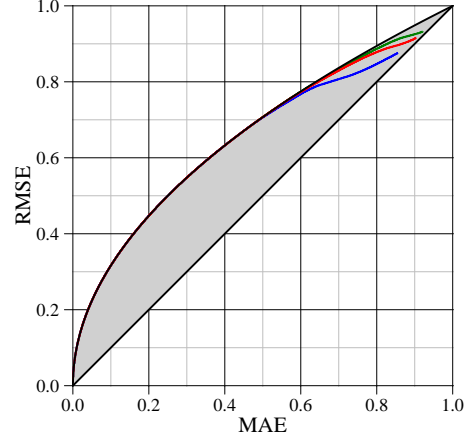


Figure 5: Bounds of the RMSE for crisp reference data (black, shaded). Above an MAE of 0.6, the soft references further restrict the range MAE and RMSE can possibly take and upper bounds for the sensitivity of the tumor classes N (green), A °II (blue), and A °III+ (red) deviate from the black maximum RMSE for crisply labelled data.

2.4. Implementation and Availability

We implemented the proposed performance measures in R [42] as package “softclassval”. The package is released under GPL 3 (<http://www.gnu.org/licenses/gpl.html>).

The project is hosted at <http://softclassval.r-forge.r-project.org> where the current development version, its check results and the source of previous versions (via the version control web interface) are available. The checks include unit tests to ensure calculational correctness, which consist of ca. twice as many lines of code than the actual function definitions. `softclassval::unittest()` executes the unit tests in interactive R sessions if package `svUnit` [43] is available.

Stable releases can conveniently be installed from the Comprehensive R Archive Network CRAN (<http://cran.r-project.org/package=softclassval>, both binaries and source code are available) by executing `install.packages("softclassval")`. Check results from CRAN for a variety of platforms can be inspected at http://cran.r-project.org/web/checks/check_results_softclassval.html.

3. Application to Astrocytoma Grading

3.1. Experimental and Data Analysis Set-Up

Experiments and Reference Labels. We prepared cryo sections of our samples which were stained for reference diagnosis (for the classes, see classifier setup below). Raman maps were recorded of the adjacent side of the remaining bulk tissue on an evenly spaced grid with step sizes between 200 and 333 μm using a fiber-optic probe with focus diameter of ca. 60 μm (order of magnitude: 10^3 cells). Figure 6a shows such a bulk sample immediately before Raman measurements.

Histological diagnosis was obtained for the parallel section (fig. 6b) and transferred to the measurement grid *without* any

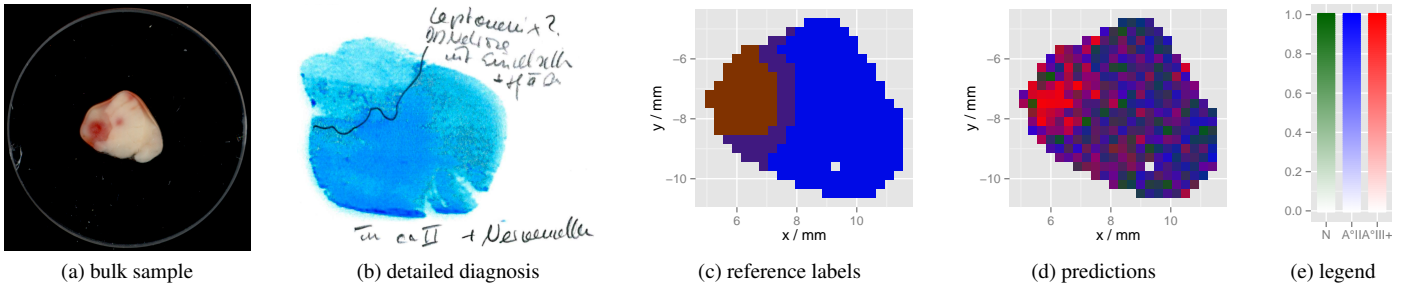


Figure 6: Samples. From left to right: (a) bulk sample ready for measurement; (b) histology results for methylene-blue stained parallel section; (c) reference labels; (d) predictions from one of the 125 cross validation iterations. The colors for reference labels and prediction are obtained by mixing the respective parts of the green (class N), blue (class A°II) and red (class A°III+) colours which stand for the pure tissues as indicated in the legend (e). Most of the sample area is diagnosed as a *mixture* of tumor °II with normal cells (reference membership: 0.1 N, 0.9 A°II, 0.0 A°III+; blue color). On the left is an area where the pathologist expressed *uncertainty*: the tissue may be either normal leptomeninges or necrotic. This uncertainty was translated to reference labels of 0.5 N, 0.0 A°II and 0.5 A°III+ (brown). A transition zone between these areas got intermediate reference labels (dark violetish). The cross validation results show some noise and decidedly lean towards necrosis for the area where the neuropathologist was uncertain.

Table 1: Overview of the data set [2]. With kind permission of Springer Science+Business Media.

class	crisp reference		crisp + soft reference	
	patients	spectra	patients	spectra
Normal	16	7 456	35	15 747
thereof controls	9	4 902	9	4 902
Astrocytoma °II	17	4 171	47	19 128
Astrocytoma °III+	27	8 279	53	21 617
total	53	19 906	80	37 015

display of the spectra (fig. 6c). Partial class memberships were used for the reference labels where ambiguity or uncertainty occurred. For example, tumor tissue between the classes (“A°II to °III”) was labeled belonging half and half to the respective classes. The diagnosis “individual tumor cells in normal tissue” and tissue where the histologist was not sure whether it contained tumor cells were labeled as 0.05 tumor and 0.95 normal, and so forth. If shape or deformation of the sample prevented the transfer of the diagnosis, the fractions of the respective areas on the reference section were used as class membership.

Figure 7 gives an overview of the pre-processed spectra immediately before centering on the average spectrum of normal grey matter. Table 1 summarizes the data set. A more detailed discussion of the samples and data set as well as spectroscopic interpretation have been given in [2].

Classifier Set-Up. The samples include a number of different tissues that were combined into the three classes requested by the neurosurgeons:

N (normal or non-tumor tissues): normal white matter, normal gray matter, and small amounts of gliotic tissue. Surgically, such tissue *must* be preserved. For convenience, we refer to this class as “normal” in the text.

A°II (low grade tumor morphology): such tissue would lead to a diagnosis of an astrocytoma °II if it is the most de-

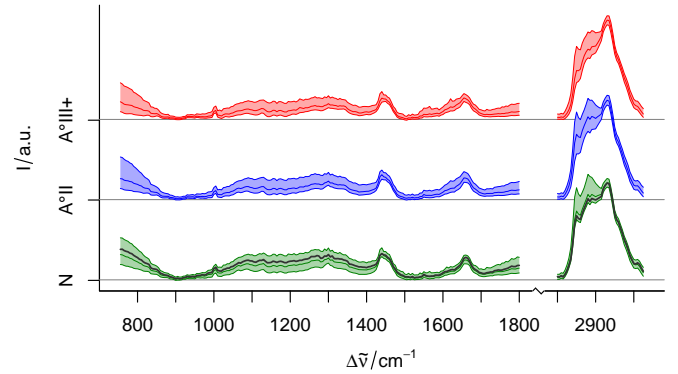


Figure 7: Weighted median, 16th, and 84th percentile spectra. Thick line: the mean grey tissue spectrum used for centering [2]. With kind permission of Springer Science+Business Media.

differentiated tissue found. Surgically, this may be thought of as “take out if possible”.

A°III+ (high grade morphology): malignant or high grade tumor tissues, comprising °III and IV morphologies as well as necrotic tissue. These tissues *must* be excised.

Note that both class boundaries are of practical importance: the boundary between normal and low grade tissues is the intended excision border. Yet, in order not to risk damage to normal brain tissue, the surgeons frequently have to back up to the border between low and high grade morphology.

The three classes are ordered with increasing malignancy. Nevertheless, we model unordered classes here, and an extension to ordered class models is outside the scope of this paper. We use here the same soft LR classifier as in [2]. Briefly, the classifier was trained using the R [42] package nnet [44]. All pre-processing was decided by spectroscopic knowledge, no data-driven steps were included and no parameter optimization was performed. However, we checked that a PLS projection

[45] of the spectra onto 25 latent variables as pre-processing for LR training did not lead to more than slight changes in the prediction (see supplementary figure S.2). 90 % of the PLS-preprocessed predictions lie within ± 0.07 of the respective predictions without PLS pre-processing. As a comparison, 90 % of the differences between different cross validation iterations for the same spectrum are within ± 0.2 . The root mean squared difference between iterations is $2.7\times$ the root mean squared difference for PLS-pre-processing with 25 latent variables.

Validation. 125 iterations of an 8-fold cross validation scheme were used, splitting the data patient-wise since spectra of one patient are not statistically independent.

Our data set does not reflect the relevant prior probabilities, nor are any such data available. Therefore, we calculate only sensitivity and specificity and do not report predictive values.

Software. Data analysis was performed in R [42] using the packages R.matlab [46] for data import, hyperSpec [47] for spectra handling, pls [48] for multiplicative signal correction of co-additions of the spectra and the PLS pre-processing for comparison, nnet [44] for the logistic regression, and ggplot2 [49] for graphical display.

3.2. Results of the Astrocytoma Grading

We report corresponding triples of one performance measure of all three classes separated by bars (N|A °II|A °III+). A tabular overview of the results is available in the supplementary material **tab. S.1**.

Best, Expected, and Worst Case Performance. Figure 8a shows the expected (product AND), best (weak AND) and worst case (strong AND) sensitivity and specificity of our models. Note that this range accounts solely for the ambiguity of the reference data. It does not account for the uncertainty due to the number of test cases nor for uncertainty due to model instability. While these uncertainties are not a topic of the present study, it may be noted that the standard deviations of the performance measures observed over the 125 iterations of the cross validation range from 0.007 to 0.013 for the sensitivities and from 0.004 to 0.006 for the specificities. For the unambiguously labeled (crisp) samples, standard deviations between 0.005 and 0.017 were observed. All these are much smaller than the symbol sizes in fig. 8a.

The expected sensitivity for the intermediate tissue morphology A °II, 0.43, is lower than the sensitivity for both normal (0.58) and high grade (0.55) morphologies. This corresponds to the A °II class also biologically being in between normal and high grade, *i. e.* the class has two borders relevant to the classification problem whereas normal and high grade classes have only one relevant border. This pattern is even stronger for the strong sensitivity (0.54|0.32|0.50), but almost vanishes for the weak sensitivity (0.62|0.57|0.62).

A similar overall pattern is observed for the expected specificities (0.82|0.69|0.80). Normal and high grade tissue are rarely confused, the difficulties in the classification lie between the consecutive classes.

The difference between strong and weak AND largely reflects the amount of ambiguity in the reference labels. This becomes clear by comparison with fig. 8b, where the overlap for ideal reconstruction of the reference data is shown. The more ambiguous the reference, the larger the gap between weak and strong performance measure: given the reference labels, the expected sensitivity for A °II cannot exceed 0.76, whereas for N and A °III+ 0.91 and 0.88 could be reached. The strong sensitivities (lower bound) cannot be more than 0.86|0.64|0.82 for the three classes. The specificity is calculated with all samples that do *not* belong to the class in the denominator, and has therefore less ambiguity. Thus expected specificities of up to 0.95|0.93|0.91 and worst-case specificities of up to 0.92|0.89|0.87 for the three classes are possible. The weak sensitivity and specificity can always reach 1.

The A °II class has soft borders to both other classes, whereas there is much less ambiguity in the reference labels between normal and high grade tissues. Class N *references* are less ambiguous than the high grade morphologies A °III+ (fig. 8b). In contrast, the *predictions* with respect to class N reach about the same sensitivity and specificity as those of class A °III+ (fig. 8a).

Fig. 9 compares the behaviour of the commonly used (crisp) sensitivity and specificity with the soft AND-operators for the crisp spectra. The specificity-sensitivity curves of the three classes were calculated using the R [42] package ROCR [50]. The band width illustrates the variation in model performance due to different composition of the training data in different iterations of the cross validation: shown are the inter quartile range and median (25th, 50th and 75th percentiles).

The primary output of the logistic regression models are posterior probabilities. As a post-processing step, the spectrum can be assigned to a class if the respective posterior probability exceeds a given threshold (hardening the prediction). To obtain the specificity-sensitivity lines, this threshold is varied.

Hardening discards small deviations that do not cross the threshold, which are therefore not detected in the specificity-sensitivity-curve. In contrast, the soft AND-operators work directly on the posterior probabilities and penalize already small deviations from the reference. This leads to the soft performance values (marked +) lying below the specificity-sensitivity-curves. The classical calculation of specificity-sensitivity-curves is possible only for crisply labelled spectra. In order to have the same test sample basis throughout the graph, soft spectra were therefore excluded from all calculations for figure 9, *i. e.* the soft performance measures are the same results marked by plus (+) signs in figure 8a. For crisp reference, all three AND-operators yield the same result as there is no ambiguity (see also fig. 3).

Hardening also influences the variance of the performance measure. On the one hand, if the hardening threshold is in the range of the predicted posterior probabilities, hardening will increase the variance on the performance measure. This causes the well-known high variance of the crisp classifier performance measures: testing with crisp class labels is described as a Bernoulli-process, leading to the variance of the observed performance $\sigma^2(\hat{p}) = \frac{p(1-p)}{n}$. The soft performance measures do

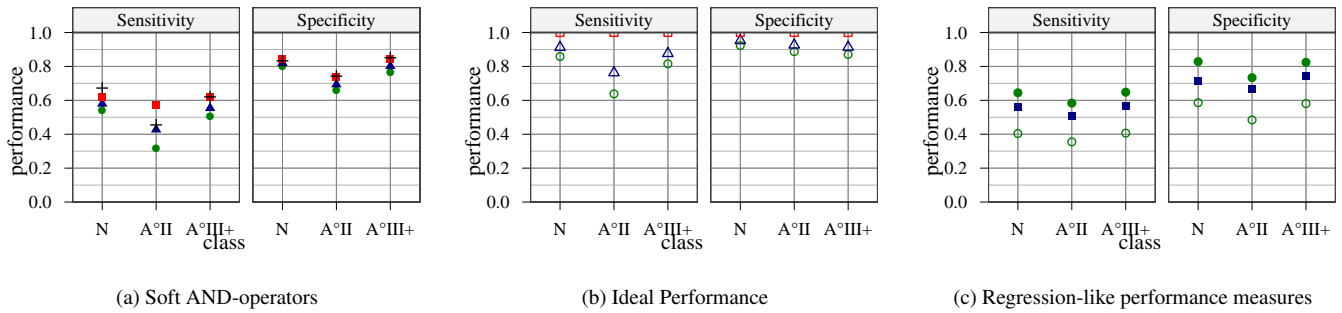


Figure 8: Results for the astrocytoma grading. (a) Expected (product; blue triangle), best (weak AND; red square) and worst case (strong AND; green circle) overlap between predicted and reference averaged over all spectra and iterations. Black crosses mark the (coinciding) results of all three operators for the crisp reference spectra. (b) The (hypothetical) results for ideal reproduction of the reference labels is shown (open symbols). (c) Performance based on the difference between prediction and reference: $1 - \text{wMAE}$ (circles) and $1 - \text{wRMSE}$ (squares). The open circles are $1 - \sqrt{\text{wMAE}}$, the lower bound of the wRMSE given the observed wMAE.

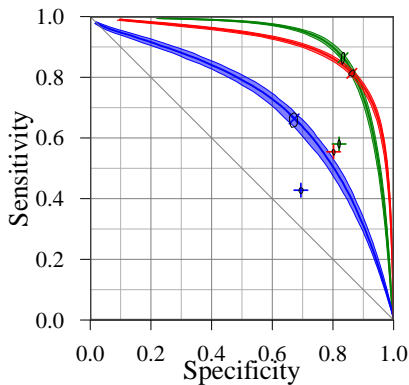


Figure 9: Specificity-sensitivity-diagram for hardened predictions of the crisp data. \times : hardening with threshold $\frac{1}{3}$. $+$: soft performance. As only crisply labelled spectra are included, all soft AND-operators coincide. Colors: green: N, blue: $A^{\circ}II$, red: $A^{\circ}III+$. The bands show the inter quartile range over the 125 cross validation iterations, thick line: median; The ROC-like lines are produced by varying the hardening threshold. Hardening discards small deviations that are penalized by the soft measures: $+$ are below the specificity-sensitivity-curves. The contours behind each \times and $+$ contain ca. 50 % of the observed values over the 125 iterations: hardening considerably increases the variance.

not suffer from this increase in variance. The increase in variance will usually be high for models that have rather gradual transitions between the classes. On the other hand, for such a model extreme thresholds will mean that (almost) all samples are on the same side of the threshold. In this (far less common) case, hardening actually lowers the variance. In our example, that would be e.g. if the $A^{\circ}II$ class were operated at sensitivity of 0.95 with a specificity of 0.10. Operating a classifier at such an extreme working point actually requires an adapted training strategy, including also an adequate composition of the training

set.

Note, however, that extreme thresholds for models that in fact predict intermediate posterior probabilities are fundamentally different from models with very sharp class transition: if the transition between the classes is immediate, hardening has hardly any effect on the variance, as the predicted posterior probabilities are already close to 0 or 1.

In our data, assigning each test sample completely to the class with the highest posterior probability (threshold $\frac{1}{n_g} = \frac{1}{3}$, working points marked \times), we observe crisp sensitivities and specificities of (0.86|0.66|0.81) and (0.83|0.67|0.86), respectively – a typical choice of working points close to the major diagonal of the specificity-sensitivity-diagram. The corresponding variances of the soft sensitivities and specificities (marked $+$) are $(1.64|0.64|0.52) \times 10^{-4}$ and $(0.16|0.36|0.21) \times 10^{-4}$ whereas the variances of the crisp performance measures are $(2.84|4.13|0.85) \times 10^{-4}$ and $(0.31|2.17|0.68) \times 10^{-4}$. In other words, this default hardening increases the variance about 60 – 550 % (sensitivity of $A^{\circ}III+$ and $A^{\circ}II$, respectively).

Hardening can thus be seen as a noise reduction technique that can be beneficial for the predictive performance. However, for the measurement of performance, information is lost. This loss becomes important in optimization of classifiers: the optimizer will not be able to distinguish well between slightly different models using any target function on the basis of hardened predictions. Even worse, the most difficult class, $A^{\circ}II$, is most affected by this avoidable increase in variance.

Figure 8c gives the results for the calibration-type performance measures. These follow the same general patterns already discussed for the direct application of the different AND-operators: specificity is higher (0.65|0.58|0.65; $1 - \text{wMAE}$) than sensitivity (0.83|0.73|0.82) and the low grade morphologies are the most difficult class. Again, the standard deviation observed over the 125 iterations is lower than the symbol size: between 0.004 and 0.013 for $1 - \text{wMAE}$ and between 0.006 and 0.012 for $1 - \text{wRMSE}$. All $1 - \text{wRMSE}$ but the specificity for normal tissue are closer to the $1 - \text{wMAE}$ than to the $1 - \sqrt{\text{wMAE}}$. This indicates small deviations from the ref-

erence for many samples rather than few grossly misclassified samples.

4. Summary and Conclusions

We propose a set of performance measures (sensitivity, specificity, predictive values, hit- or error rates, etc.) that can be calculated for classifiers with continuous outcome without the need of “hardening”.

Ambiguity of the reference of cases that are borderline according to the ground truth or gold standard diagnosis leads to ambiguity in the measured performance as well. The proposed measures reflect this as worst case (strong AND), best case (weak AND) and expected (product AND) performance.

Deviations from the reference can also be evaluated using weighted versions of well-known calibration performance measures, namely the weighted mean absolute error wMAE and the weighted root mean squared error wRMSE. Their comparison in addition allows to distinguish situations with many small deviations from few large errors.

Our new measures improve their classical counterparts in four different ways:

1. While classification assumes perfectly distinct classes, in reality this is often not the case. In the past, samples with ambiguous reference labels (borderline cases) usually were excluded completely from both classifier training and testing, or their reference labels were hardened. This has serious consequences. Excluding borderline cases from classifier training can lead to overestimation of class separability, while hardening of class labels samples truly in between the classes (*e. g.* mixed cell population or cell population currently undergoing de-differentiation) will actually drive the model to overestimate class separability. However, as the classical performance measures do not allow to evaluate the model performance for borderline cases, this overoptimistic modeling of class separation could not be detected, the same is true if the reference labels were hardened. If the predictions are hardened as well, neither can under-estimation of class separability be detected. Excluding borderline cases leaves the validation completely blind for the behaviour of the classifier close to the class boundaries defined by the reference. Hardened reference labels probe this region, but high variance results. In contrast, the soft performance measures penalize over- or underestimation of class separability and have lower variance than their hardened counterparts. They thus open the way for more realistic modeling of class boundaries that uses also borderline training cases.
2. Truly ambiguous samples may be the actual target of a classifier, such as in our example of astrocytoma grading for surgical guidance. In that case, borderline cases are *most important* test samples, since testing clear cases only cannot be considered representative for the application. The proposed soft measures work with samples diagnosed as borderline cases and thus allow for more realistic classifier testing.
3. Hardening of the outcome has (like other dichotomization approaches) been criticized due to the inherent loss of information. This causes difficulties when classifier performance is compared. Model optimization relies on detecting already small differences in the predictive ability of the models which is thwarted by the hardening. In contrast, the soft performance measures already report small deviations from the reference and thus allow to differentiate between more similar models than their crisp counterparts.
4. For models with gradual class transitions (*i.e.* that actually predict intermediate posterior probability values), typical hardening thresholds lead to an increase in variance that is avoided by the soft performance measures. For our astrocytoma grading, the sensitivity and specificity based on the soft AND-operators show between 39 and 84 % less variance over the 125 iterations of the 8-fold cross validation than sensitivity and specificity based on crisp classification.

Acknowledgments

Financial support by the Associazione per i Bambini Chirurgici del Burlo (IRCCS Burlo Garofolo Trieste) is highly acknowledged.

References

- [1] K. H. Esbensen, P. Geladi, [Principles of Proper Validation: use and abuse of re-sampling for validation](#), J. Chemometrics 24 (3-4) (2010) 168–187.
- [2] C. Beleites, K. Geiger, M. Kirsch, S. B. Sobottka, G. Schackert, R. Salzer, [Raman spectroscopic grading of astrocytoma tissues: using soft reference information.](#), Anal Bioanal Chem 400 (9) (2011) 2801–2816. doi:10.1007/s00216-011-4985-4.
- [3] S. R. VandenBerg, [Current diagnostic concepts of astrocytic tumors.](#), Journal of neuropathology and experimental neurology 51 (6) (1992) 644–657.
- [4] D. N. Louis, H. Ohgaki, O. D. Wiestler, W. K. Cavenee, P. C. Burger, A. Jouvet, B. W. Scheithauer, P. Kleihues, [The 2007 WHO classification of tumours of the central nervous system.](#), Acta neuropathologica 114 (2) (2007) 97–109. doi:10.1007/s00401-007-0243-4.
- [5] J. M. Kros, T. Gorlia, M. C. Kouwenhoven, P.-P. Zheng, V. P. Collins, D. Figarella-Branger, F. Giangaspero, C. Giannini, K. Mokhtari, S. J. Mørk, A. Paetau, G. Reifenberger, M. J. van den Bent, [Panel review of anaplastic oligodendroglioma from European Organization For Research and Treatment of Cancer Trial 26951: assessment of consensus in diagnosis, influence of 1p/19q loss, and correlations with outcome.](#), Journal of neuropathology and experimental neurology 66 (6) (2007) 545–551. doi:10.1097/01.jnen.0000263869.84188.72.
- [6] I. Duran, J. J. Raizer, [Low-grade gliomas: management issues.](#), Expert review of anticancer therapy 7 (12 Suppl) (2007) S15–S21. doi:10.1586/14737140.7.12s.S15.
- [7] R. Stupp, M. Reni, G. Gatta, E. Mazza, C. Vecht, [Anaplastic astrocytoma in adults](#), Critical Reviews in Oncology/Hematology 63 (1) (2007) 72–80.
- [8] D. Moskopp, H. Wassmann (Eds.), [Neurochirurgie](#), Schattauer, 2004, Ch. Intrakranielle Tumoren, pp. 407 – 488.
- [9] J. A. Schwartzbaum, J. L. Fisher, K. D. Aldape, M. Wrensch, [Epidemiology and molecular pathology of glioma.](#), Nat Clin Pract Neurol 2 (9) (2006) 494–503; quiz 1 p following 516. doi:10.1038/ncpneuro0289.
- [10] N. F. Marko, J. Quackenbush, R. J. Weil, [Why is there a lack of consensus on molecular subgroups of glioblastoma? Understanding the nature of biological and statistical variability in glioblastoma expression data.](#), PLoS One 6 (7) (2011) e20826. doi:10.1371/journal.pone.0020826.

- [11] R. G. Brereton, One-class classifiers, *Journal of Chemometrics* 25 (2011) 225–246. doi:10.1002/cem.1397.
- [12] R. Brereton, *Chemometrics for pattern recognition*, Wiley, Chichester, U.K, 2009.
- [13] D. M. Tax, One-class classification – Concept-learning in the absence of counter-examples, Ph.D. thesis, Technische Universiteit Delft (2001).
- [14] G. M. Foody, *Status of land cover classification accuracy assessment*, *Remote Sensing of Environment* 80 (1) (2002) 185–201.
- [15] E. Binaghi, P. A. Brivio, P. Ghezzi, A. Rampini, *A fuzzy set-based accuracy assessment of soft classification*, *Pattern Recognition Letters* 20 (9) (1999) 935–948.
- [16] R. G. Pontius, M. L. Cheuk, *A generalized cross-tabulation matrix to compare soft-classified maps at multiple resolutions*, *International Journal of Geographical Information Science* 20 (1) (2006) 1–30.
- [17] J. Silván-Cárdenas, L. Wang, *Sub-pixel confusion-uncertainty matrix for assessing soft classifications*, *Remote Sensing of Environment* 112 (3) (2008) 1081–1095. doi:10.1016/j.rse.2007.07.017.
- [18] J. Chen, X. Zhu, H. Imura, X. Chen, *Consistency of accuracy assessment indices for soft classification: Simulation analysis*, *ISPRS Journal of Photogrammetry and Remote Sensing* 65 (2) (2010) 156–164. doi:10.1016/j.isprsjprs.2009.10.003.
- [19] S. Wold, M. Sjöström, *SIMCA: A Method for Analyzing Chemical Data in Terms of Similarity and Analogy*, 1977, Ch. 13, pp. 243–282. arXiv:http://pubs.acs.org/doi/pdf/10.1021/bk-1977-0052.ch012, doi:10.1021/bk-1977-0052.ch012.
- [20] A. de Juan, M. Mäder, M. Martínez, R. Tauler, *Combining hard- and soft-modelling to solve kinetic problems*, *Combining hard- and soft-modelling to solve kinetic problems* 54 (2000) 123–141. doi:10.1016/S0169-7439(00)00112-X.
- [21] K. Varmuza, *Introduction to multivariate statistical analysis in chemometrics*, CRC Press, Boca Raton, 2009.
- [22] P. Oliveri, G. Downey, *Multivariate class modeling for the verification of food-authenticity claims*, *Trends in Analytical Chemistry* 35 (2012) 74–86. doi:10.1016/j.trac.2012.02.005.
- [23] C. Krafft, L. Shapoval, S. B. Sobottka, K. D. Geiger, G. Schackert, R. Salzer, *Identification of primary tumors of brain metastases by SIMCA classification of IR spectroscopic images.*, *Biochimica et Biophysica Acta* 1758 (7) (2006) 883–891. doi:10.1016/j.bbame.2006.05.001.
- [24] M. Khanmohammadi, A. B. Garmarudi, K. Ghasemi, H. K. Jaliseh, A. Kaviani, *Diagnosis of colon cancer by attenuated total reflectance-Fourier transform infrared microspectroscopy and soft independent modeling of class analogy.*, *Med Oncol* 26 (3) (2009) 292–297. doi:10.1007/s12032-008-9118-3.
- [25] P. Heraud, B. R. Wood, J. Beardall, D. McNaughton, *Effects of pre-processing of Raman spectra on in vivo classification of nutrient status of microalgal cells*, *Journal of Chemometrics* 20 (2006) 193–197. doi:10.1002/cem.990.
- [26] R. G. Brereton, G. R. Lloyd, *Support vector machines for classification and regression.*, *Analyst* 135 (2) (2010) 230–267. doi:10.1039/b918972f.
- [27] P. Lasch, W. Haensch, D. Naumann, M. Diem, *Imaging of colorectal adenocarcinoma using FT-IR microspectroscopy and cluster analysis.*, *Biochimica et Biophysica Acta* 1688 (2) (2004) 176–186. doi:10.1016/j.bbadis.2003.12.006.
- [28] W. Steller, J. Einkenkel, L.-C. Horn, U.-D. Braumann, H. Binder, R. Salzer, C. Krafft, *Delimitation of squamous cell cervical carcinoma using infrared microspectroscopic imaging.*, *Analytical and Bioanalytical Chemistry* 384 (1) (2006) 145–154. doi:10.1007/s00216-005-0124-4.
- [29] C. Krafft, G. Steiner, C. Beleites, R. Salzer, *Disease recognition by infrared and Raman spectroscopy.*, *Journal of Biophotonics* 2 (1-2) (2009) 13–28. doi:10.1002/jbio.200810024.
- [30] A. Bonifacio, C. Beleites, F. Vittur, E. Marsich, S. Semeraro, S. Paoletti, V. Sergo, *Chemical imaging of articular cartilage sections with Raman mapping, employing uni- and multi-variate methods for data analysis.*, *Analyst* 135 (12) (2010) 3193–3204. doi:10.1039/c0an00459f.
- [31] V. Fedorov, F. Mannino, R. Zhang, *Consequences of dichotomization*, *Pharmaceutical Statistics* 8 (2009) 50–61. doi:10.1002/pst.331.
- [32] C. Kendall, N. Stone, N. Shepherd, K. Geboes, B. Warren, R. Bennett, H. Barr, *Raman spectroscopy, a potential tool for the objective identification and classification of neoplasia in Barrett’s oesophagus.*, *The Journal of pathology* 200 (5) (2003) 602–609. doi:10.1002/path.1376.
- [33] S. Ellison, T. Fearn, *Characterising the performance of qualitative analytical methods: Statistics and terminology*, *TrAC Trends in Analytical Chemistry* 24 (6) (2005) 468–476.
- [34] R. N. Forthofer, E. S. Lee, *Introduction to biostatistics - a guide to design, analysis and discovery*, Academic Press, 1995. doi:ISBN0-12-262270-7.
- [35] S. Gottwald, *Many-Valued Logic*, in: E. N. Zalta (Ed.), *The Stanford Encyclopedia of Philosophy*, spring 2010 Edition, 2010.
- [36] P. Hajek, *Fuzzy Logic*, in: E. N. Zalta (Ed.), *The Stanford Encyclopedia of Philosophy*, fall 2010 Edition, 2010.
- [37] D. Dubois, H. Prade, *A review of fuzzy set aggregation connectives*, *Information sciences* 36 (1-2) (1985) 85–121.
- [38] J. Pontius, Robert Gilmore, J. Connors, *Expanding the conceptual, mathematical and practical methods for map comparison*, in: M. Caetano, M. Painho (Eds.), *7th International Symposium on Spatial Accuracy Assessment in Natural Resources and Environmental Sciences*, *Proceedings of Accuracy 2006*, 2006, plenary lecture.
- [39] H. Reichenbach, *Wahrscheinlichkeitslogik*, *Erkenntnis* 5 (1935) 37–43.
- [40] H. G. Lewis, M. Brown, *A generalized confusion matrix for assessing area estimates from remotely sensed data*, *International journal of remote sensing* 22 (16) (2001) 3223–3235.
- [41] G. W. Brier, *Verification of Forecasts Expressed in Terms of Probability*, *Monthly Weather Review* 78 (1) (1950) 1–3.
- [42] R Development Core Team, *R: A Language and Environment for Statistical Computing*, R Foundation for Statistical Computing, Vienna, Austria, ISBN 3-900051-07-0 (2011).
- [43] P. Grosjean, *SciViews-R: A GUI API for R*, UMONS, MONS, Belgium (2012).
- [44] W. N. Venables, B. D. Ripley, *Modern Applied Statistics with S*, 4th Edition, Springer, New York, 2002.
- [45] R. Wehrens, B.-H. Mevik, *pls: Partial Least Squares Regression (PLSR) and Principal Component Regression (PCR)*, R package version 2.1-0 (2007).
- [46] H. Bengtsson, J. Riedy, *R.matlab: Read and write of MAT files together with R-to-Matlab connectivity*, R package version 1.2.4 (2008).
- [47] C. Beleites, V. Sergo, *hyperSpec: a package to handle hyperspectral data sets in R*, *Journal of Statistical Software in preparation* R package version 0.98-20121028.
- [48] B.-H. Mevik, R. Wehrens, *The pls Package: Principal Component and Partial Least Squares Regression in R*, *Journal of Statistical Software* 18 (2) (2007) 1 – 24.
- [49] H. Wickham, *ggplot2: elegant graphics for data analysis*, Springer New York, 2009.
- [50] T. Sing, O. Sander, N. Beerwinkel, T. Lengauer, *ROCR: Visualizing the performance of scoring classifiers.*, R package version 1.0-4 (2009).
- [51] C. Beleites, U. Neugebauer, T. Bocklitz, C. Krafft, J. Popp, *Sample Size Planning for Classification Models* arXiv:1211.1323, doi:10.1016/j.aca.2012.11.007.

Supplementary Material

Table S.1: Results for the Astrocytoma Grading using soft LR.

(a) The different AND-operators. The last three columns (“ideal”) give the best possible performance that can be obtained with the given reference, i. e. the result if the prediction equals the reference memberships.

performance	class		LR-soft				ideal		
			strong	prd	weak	(crisp)	strong	prd	weak
sens	N	\bar{x}	0.541	0.580	0.620	0.672	0.859	0.913	1.000
		$s(x)$	0.013	0.013	0.013	0.017			
	A°II	\bar{x}	0.315	0.428	0.570	0.455	0.638	0.763	1.000
		$s(x)$	0.007	0.008	0.009	0.012			
	A°III+	\bar{x}	0.504	0.554	0.617	0.620	0.815	0.876	1.000
		$s(x)$	0.007	0.007	0.008	0.008			
spec	N	\bar{x}	0.799	0.820	0.842	0.833	0.923	0.953	1.000
		$s(x)$	0.004	0.004	0.004	0.005			
	A°II	\bar{x}	0.659	0.694	0.738	0.742	0.888	0.926	1.000
		$s(x)$	0.006	0.006	0.006	0.009			
	A°III+	\bar{x}	0.767	0.802	0.846	0.851	0.871	0.914	1.000
		$s(x)$	0.005	0.005	0.005	0.005			

(b) The regression-type operators.

performance	class		LR-soft		
			1 – wMAE	1 – wRMAE	1 – wRMSE
sens	N	\bar{x}	0.645	0.404	0.563
		$s(x)$	0.013	0.011	0.012
	A°II	\bar{x}	0.584	0.355	0.508
		$s(x)$	0.007	0.006	0.007
	A°III+	\bar{x}	0.648	0.407	0.568
		$s(x)$	0.006	0.005	0.006
spec	N	\bar{x}	0.829	0.586	0.712
		$s(x)$	0.004	0.005	0.006
	A°II	\bar{x}	0.734	0.484	0.664
		$s(x)$	0.006	0.006	0.006
	A°III+	\bar{x}	0.824	0.581	0.744
		$s(x)$	0.004	0.005	0.006

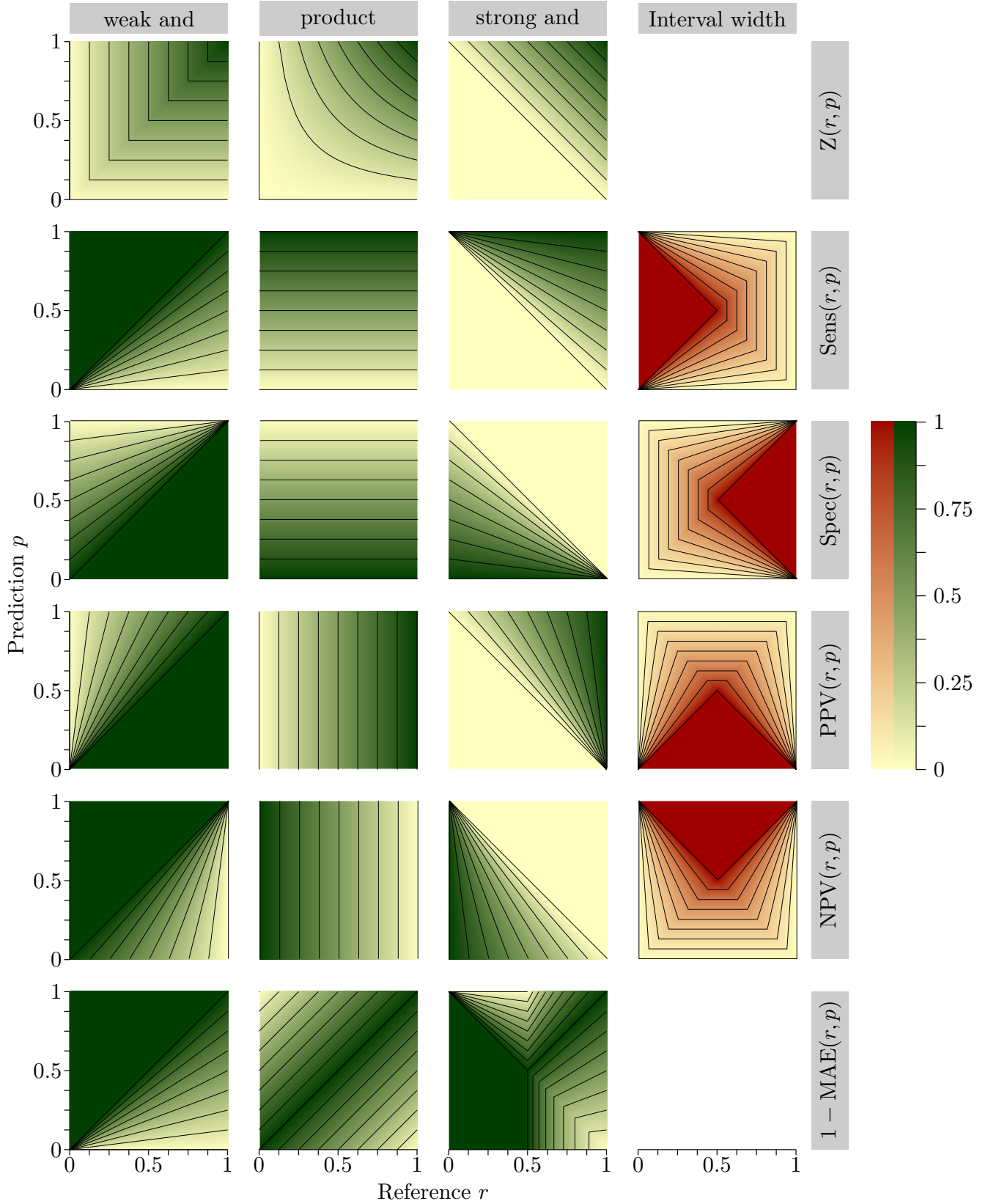


Figure S.1: The values (color) of the three operators (columns) and the soft performance measures (rows) for a single sample as function of reference and prediction. The 4th column (red) gives the width of the interval between strong and weak measures. The interval ranges from 0 to 1 for the triangle between the side where the crisp measure is not defined and the center of the input space ($r = 0.5; p = 0.5$). Note the symmetry between the performance measures (compare also fig. 1f). Z^{prod} are similar to Z^{weak} for small values and similar to Z^{strong} for high values.

The last row gives the MAE-version of the sensitivity.

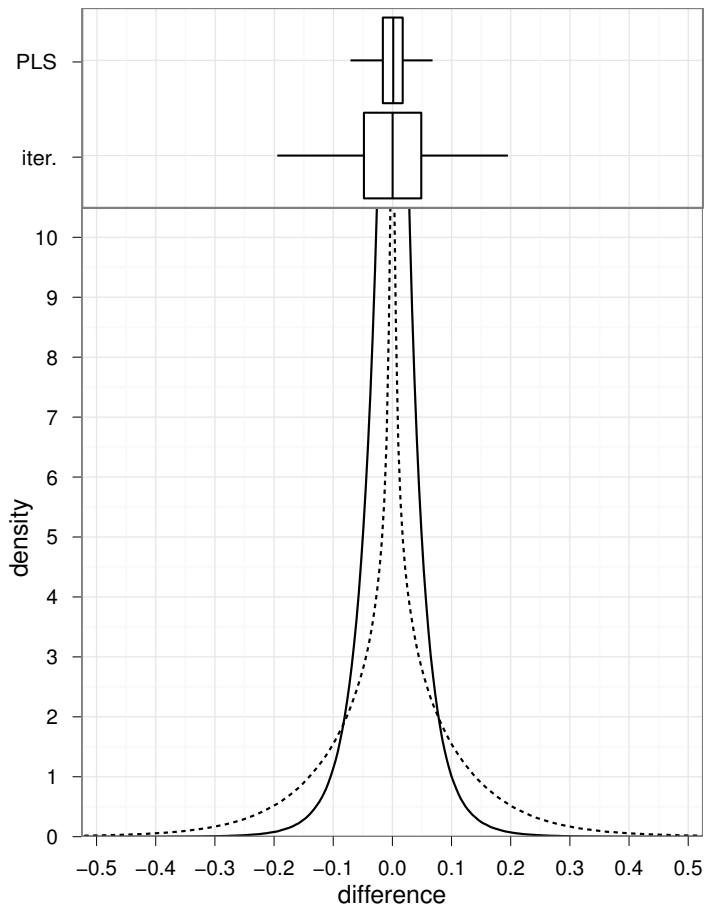


Figure S.2: Distribution of differences in the prediction between classifiers with and without 25 LV PLS as pre-processing (LR vs. PLS-LR, same iteration). To better compare the results, the distribution of differences between the iterations of the LR (without PLS) are shown as well (dotted) line. 90% of the PLS-preprocessed predictions lie within ± 0.07 of the respective predictions without PLS pre-processing, whereas the 5th to 95th percentile of the between-iteration differences range from -0.2 to +0.2.